Journal of Software Engineering, 2015
ISSN 1819-4311 / DOI: 10.3923/jse.2015.

Identification of Conifer Species Based on Laboratory Spectroscopy and an Artificial Neural Network

Xin Wang, Yi Zeng, Shaohuang Wang and Tianzhong Zhao
College of Information Science and Technology, Beijing Forestry University, Beijing, 100083, China

Corresponding Author: Tianzhong Zhao, College of Information Science and Technology, Beijing Forestry University, Beijing, 100083, China

ABSTRACT

Remote identification of individual tree species contributing to a forest's ecosystem is essential for the proper utilization and protection of our forest resources. In this study, we propose a novel neural network method, termed LAP-BP (which modifies the standard BP algorithm using the Laplace Transform function) to be able to discern individual tree species from one another based on their spectral imaging. To accomplish this, hyperspectral data (with a spectral range of 350~2,500 nm) in combination with the modified LAP-BP method was used in the identification of five common coniferous species endemic to China. Results show that when the value of the hidden layer of the neural network, in conjunction with training objective, is (6, 9) that LAP-BP network achieves the highest accuracy in coniferous species identification with a prediction accuracy of 86.78%. The differences of leaf thickness and shape among the five coniferous species are the primary factors contributing to the different spectral separabilities. This study offers a reference for new ideas and a novel methodology in coniferous species identification.

Key words: Artificial neural network, Laplace function, principal component analysis, supervision classification, hyperspectral data analysis

INTRODUCTION

Hyperspectral remote sensing technology is one of the major technological breakthroughs used in land observation since the 1980s. It can provide more detailed spectral information of ground objects as compared with multispectral remote sensing technology and offers effective approaches for research on subtle features of ground objects. Hyperspectral remote-sensing data is significantly featured as: (1) Multiple spectral bands-every pixel can be supplied with dozens, hundreds and even thousands of spectral bands depending on the program (e.g., AVIRIS has 224 spectral bands in the spectral range of 0.4~2.5 μm), (2) Narrow band widths-the band widths are usually less than 10 nm, which results in an extremely high spectral resolution of hyperspectral remote-sensing data, (3) Contiguous spectral bands-some sensors can provide a nearly contiguous ground spectrum within the solar spectrum of 350~2500 nm (known as the unification of spectrum and pixel), which is one of most significant characteristics of hyperspectral remote-sensing data because it allows for the operator to have no prior knowledge of the sample before use, (4) Very large data size-data size largely increases with an increase in the number of spectral bands and (5) Large information redundancy-since neighboring reflectance are correlated, information redundancy is relatively high (Zhao, 2003; Zhang and Zhang, 2005).

As one of the major renewable resources of the earth and the main body of the continental ecosystem, forests provide rich material resources for long term human existence and development

and plays an extremely important role in maintaining ecological processes and balance (Zhang *et al.*, 2007). Correct identification of the populations of tree species that comprise a forest's ecosystem is the basis for proper utilization and protection of forest resources (Liu and Zhang, 2004). Conventional survey and identification methods for distinguishing forest tree species mainly rely on high-cost, time and energy consuming field surveys (tree species classification is morphologically implemented, i.e., through external morphological characteristics such as stem, leaf, flower and fruit to identify the type of tree) and/or large-scale air photo data for interpretation.

In the last 20-30 years, application studies on the identification of forest tree species by space remote sensing data (e.g., TM, SPOT) has been restricted to spectral resolution of multi-spectral remote sensing. Tree species with similar spectral curves are hard to distinguish between and can only be divided as vegetation or non-vegetation. Often these forest regions are simply divided as needle leaves and broad leaves. These classifications cannot possibly meet the requirements of actual production (Zhang, 2007; Tan, 2003, 2008; Dang, 2000). This lack of separation is determined by the following two factors: (1) A lack of hyperspectral resolution and broad spectral bands results in different trees often having extremely similar spectral characteristics; their subtle spectral differences simply can not be detected by sensing data with such wide spectral bands and (2) Illumination process on which optical remote sensing relies upon is inconstant, often leading to significantly different spectral characteristics even within the same tree species.

Hyperspectral remote sensing breaks through the limitations caused by spectral resolution. Currently, the hyperspectral remote sensing technique is being widely used for vegetation research. Compared to multi-spectral data it can not only effectively improve species classification precision (Tan, 2003), but it can also estimate chemical components of vegetations (such as N, P and K saccharides, starch, protein, cellulose and chlorophyll, etc.), which are all found in the leaves of vegetation (Zhang *et al.*, 1997), evaluate vegetation growth and assess vegetation biomass (Pu and Gong, 2000). There are many successful examples of the use of hyperspectral remote sensing in the identification of plant and tree species. For instance Pu and Gong (2000) used (CASI) Compact Airborne Spectrographic Imager data and designed a vegetation exponent-based estimation and forecasting method for invasive plant species identification. Similarly Zhang *et al.* (1997) also utilized hyperspectrum for tree species identification. Therefore, hyperspectral data can detect the types of ground objects with subtle spectral differences and significantly improves the identification accuracy for forest tree species (Martin *et al.*, 1998; Tan *et al.*, 2005), thus providing the basis for the most powerful method currently available in the acquisition of more precise forest population distributions.

Hyperspectral remote sensing has benefited greatly from multidisciplinary and interdisciplinary analysis techniques such as neural networking, genetic algorithms, fuzzy mathematics and SVM (Support Vector Machine). These tools have been applied towards pattern identification in order to form a series of new methods. Of these, neural network-based methods is one of methods used in the field (Wang and Zhang, 1998; Zhang and Shao, 2002; Qi and Zhang, 2007; Wu *et al.*, 2007; Zhang *et al.*, 2008; Pu *et al.*, 2008). The comprehensive analysis capability of artificial neural network models provides a reliable method in the evaluation and classification of remote sensing and multi-source data. Therefore, neural networks provide a promising application prospect in the efficient classification of tree populations.

In this study, we proposed an identification method for coniferous tree species utilizing hyperspectral data. We initially selected three principal component bands from X pieces of bands

using the (PCA) Principal Component Analysis. These bands were then analyzed using Laplace as the neural network algorithm for activation function in the identification of coniferous tree species. Experimental results show that five tree species (black pine, masson pine, slash pine, cedar and *Pseudolarix* coulc) can be effectively distinguished by this method.

MATERIALS AND METHODS

Data collection: The experimental site was the botanic garden on the Zhejiang A and F University campus, located in Lin'an City, Zhejiang province, China. Five coniferous tree species (black pine, masson pine, slash pine, cedar and *Pseudolarix*) were chosen for the experiment and five separate trees were selected from each species. From these, leaves at different ages in the same tree may exhibit distinctive spectral characteristics. Ten mature leaf samples were randomly collected from each plant to account for spectral variation. A total of 48, 49, 47, 49 and 44 leaf samples were collected, respectively. Field sampling was carried out on clear days, in which leaves from lush trees were collected and stored in a preservation box and immediately took indoors for spectrum measurement with the field spectrum radiometer ASD Field Spec Pro FR. The band of the radiometer ranges was from 350-2,500 nm with 2,151 bands in total. A high-density vegetation probe, matched with the radiometer, was used to ensure the accuracy and stability of the spectrum measurements. Furthermore, a standard whiteboard calibration was conducted on every ten leaves measured. Each leaf was repeatedly measured ten times and then we took the mean value as the spectral reflectance value for each leaf. Leaves and spectral curves of the five coniferous tree species are shown in Fig. 1 and 2.

Methods

PCA (principal component analysis): For the sample, observe n pieces of variables which are X_1, X_2, ..., X_p of the data matrix of n pieces of samples:

$$\begin{pmatrix} x_{11} & \cdots & x_{1p} \\ \vdots & \ddots & \vdots \\ x_{n1} & \cdots & x_{np} \end{pmatrix}$$

Fig. 1(a-e): Leaves of (a) Black pine, (b) Masson pine (c) Slash pine, (d) Cedar and (e) *Pseudolarix*

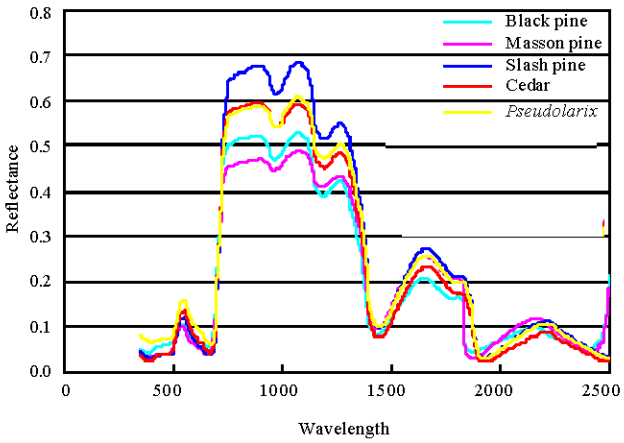

Fig. 2: Spectral curves of five coniferous tree species

Where:

$$x_j = \begin{pmatrix} x_{1j} \\ x_{2j} \\ \vdots \\ x_{nj} \end{pmatrix}, j = 1, 2, \cdots, p$$

PCA is a method that synthesizes p pieces of observed variables into p pieces of new variables (aggregate variables), defined as:

$$\begin{cases} F_1 = a_{11}x_1 + a_{12}x_2 + \cdots + a_{1p}x_p \\ F_2 = a_{21}x_1 + a_{22}x_2 + \cdots + a_{2p}x_p \\ \vdots \\ F_p = a_{p1}x_1 + a_{p2}x_2 + \cdots + a_{pp}x_p \end{cases}$$

It can be written for short as:

$$F_j = a_{j1}x_1 + a_{j2}x_2 + \ldots + a_{jp}x_p \quad j = 1, 2, \ldots, p$$

The model is required to fit with the following conditions:

- F_i, F_j are uncorrelated ($i \neq j$, $i, j = 1, 2, \ldots, p$)
- Variance of F_1>variance of F_2>variance of F_3 and so on
- $a_{k1}^2 + a_{k2}^2 + \cdots + a_{kp}^2 = 1, \ k = 1, 2, \cdots, \ p$

Hence, F_1 is referred as the first principal component, F_2 is referred as the second principal component and so on, there are n pieces of principal components. The a_{ij} is referred as principal component coefficient.

Jeffries-Matusita (JM) distance: The Jeffries-Matusita (JM) distance can determine separability among samples with a parameter value between 0 and 2.0. The parameter value indicates the capacities of separability between the selected regions of interest; a value higher than 1.9 illustrates a good separability. The calculation equation is as follows:

$$JM_{cd} = 2\times\left(1-e^{-Bhat_{cd}}\right)$$

where, $Bhat_{cd}$ is the Bhattacharyya distance and the calculation equation is:

$$Bhat_{cd} = \frac{1}{8}(M_c - M_d)^T\left(\frac{V_c + V_d}{2}\right)^{-1}(M_c - M_d) + \frac{1}{2}\log_e\left[\frac{\frac{V_c + V_d}{2}}{\sqrt{(|V_c|\times|V_d|)}}\right]$$

where, c and d represent two different species, respectively; M_c, M_d, V_c and V_d individually represents the mean value and a covariance matrix of c and d.

Introduction of LAP-BP algorithm: Standard BP algorithms have disadvantages, primarily slow convergence rates of the learning algorithm and a poor generalization capability of the neural network (Yuan, 1999; Dang, 2000). In view of the above defects, scholars have improved the BP algorithm from different perspectives; a new activation function and its combination is one of the improved methods commonly used. A previous study proposed a family of activation functions with a first derivative of $\sec h^n(x)$, n = 1, 2,···. When compared with the standard Sigmoid function it was observed that part of the family of activation functions can significantly improve the convergence rate of the neural network. Additionally, Wu and Zhao (2001) and Shen and Wang (2003) proposed novel activation function of neural networks model according to instance verification and the variable model of activation function obtained with fast convergence speed, respectively. In summary, improvement of the activation function can increase the convergence rate of the neural network.

In this study, the Laplace function was used as an activation function for improving the standard BP algorithm (Laplace-Back Propagation Neural Network, LAP-BP). As a non-elementary function, Laplace has been widely used in probability, statistics and partial differential equation. Its (CDF) Cumulative Distribution Function is as follows:

$$\begin{cases}\frac{1}{2}\exp(-\frac{u-x}{\lambda}) & \text{if} x < u\\ 1-\frac{1}{2}\exp(-\frac{x-u}{\lambda}) & \text{if} x \geq u\end{cases}$$

where, μ is location parameter, λ>0 is scale parameter. λ rectifies the gradient of function with its first derivative, i.e., its probability density function of:

$$\frac{1}{2\lambda}\begin{cases}\exp(-\frac{u-x}{\lambda}) & \text{if} x < u\\ \exp(-\frac{x-u}{\lambda}) & \text{if} x \geq u\end{cases}$$

Graph of Laplace function is presented in Fig. 3.

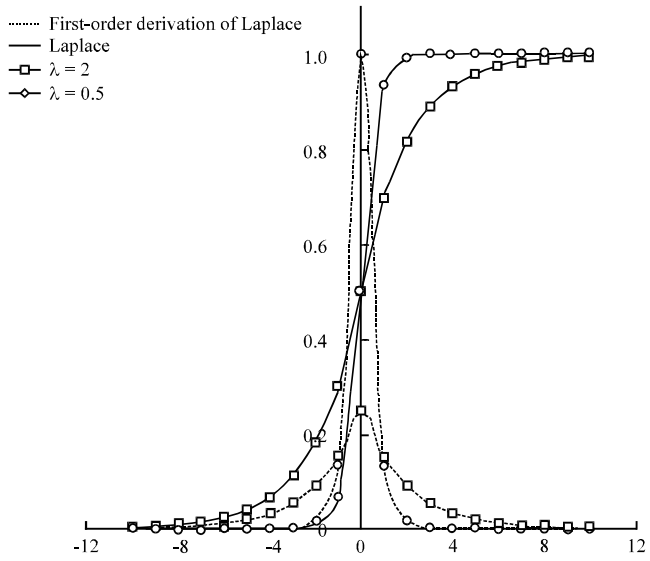

Fig. 3: Graph of Laplace function and its first derivative

The LAP-BP neural network refers to the application of the Laplace function of new activation to BP neural network. In other words, substitute the CDF of Laplace function and its first derivative for the standard BP algorithm activation function and its first derivative. The calculations are:

- The output algorithm of output node(x<u)
- Output of hidden node:

$$y^{(k)} = \begin{cases} \frac{1}{2}\exp(-\frac{u - X^{(k)} * IW}{\lambda}) & \text{if} X^{(k)} * IW < u \\ 1-\frac{1}{2}\exp(-\frac{X^{(k)} * IW - u}{\lambda}) & \text{if} X^{(k)} * IW \geq u \end{cases}$$

Output of output node:

$$O^{(k)} = \begin{cases} \frac{1}{2}\exp(-\frac{u - y^{(k)} * LW}{\lambda}) & \text{if} y^{(k)} * LW < u \\ 1-\frac{1}{2}\exp(-\frac{y^{(k)} * LW - u}{\lambda}) & \text{if} y^{(k)} * LW \geq u \end{cases}$$

where, $X^{(k)}$ represents the kth sample, k = 1, 2, ..., n; $y^{(k)}$ represents output of hidden node; $O^{(k)}$ represents the output of the output node; IW represents connection weight (including threshold) between the input layer and the hidden layer; LW IW represents connection weight (including threshold) between the hidden layer and the output layer and μ, λ are parameters of the Laplace function.

Error correction algorithm for output layer (from hidden layer to output layer):

Error equation:

$$\delta^{(k)} = (t^{(k)} - O^{(k)}) * \frac{1}{2\lambda} \begin{cases} \exp(-\frac{u - y^{(k)} * LW}{\lambda}) \text{ if } y^{(k)} * LW < u \\ \exp(-\frac{y^{(k)} * LW - u}{\lambda}) \text{if } y^{(k)} * LW \geq u \end{cases}$$

where, $\delta^{(k)}$ represents the error correction value of the kth sample in the output layer; $t^{(k)}$ represents the desired output of the kth sample of the output node.

Error correction algorithm for the layer of hidden node (from input node to hidden node):

Error equation:

$$\varphi_{\bullet h}^{(k)} = \delta^{(k)} LW'_{h\bullet} * \frac{1}{2\lambda} \begin{cases} \exp(-\frac{u - \gamma_{\bullet h}}{\lambda}) \text{ if } \gamma_{\bullet h} < u \\ \exp(-\frac{\gamma_{\bullet h} - u}{\lambda}) \text{if } \gamma_{\bullet h} \geq u, \ h = 2,3,\cdots q+1, \end{cases}$$

where, $\gamma = X^{(k)} * IW$, $\varphi_{\bullet h}^{(k)}$ represents the value of the hth column of error correction values of the kth sample in the hidden layer, $LW'_{h\bullet}$ represents the transposition of the hth row of the connection weight (including threshold) between the hidden layer and the output layer. $\gamma_{\bullet h}$ represents the value of the hth column of the weighted products of the kth sample and IW.

Experiments: In this study, 237 hyperspectral data of black pine, masson pine, slash pine, cedar and *Pseudolarix* were investigated (Table 1).

A total of 2151 spectral bands were analyzed using PCA and the numbers of major components, according to their cumulative variance contribution rates, were selected; a greater contribution rate indicates an increase in the strength of the original variable included in the principal component. We found that when the number of major components equaled 3 that the contribution rate reached 95.26%, therefore 3 major components were selected for the identification of coniferous tree species. This can guarantee that the maximum amount of information from the original variables is contained in the aggregate variable.

According to a three-dimensional space diagram of the 3 major components of the five coniferous tree species a preferable separability was shown (Fig. 4). JM distance is used as an evaluation criterion in order to evaluate the separability of the three major components mentioned above for the five species of pine trees. Table 2 lists the JM values of the five species of pine trees (i.e., the mean value of the JM values between any two of black pine, masson pine, slash pine, cedar and *Pseudolarix*). According to Table 2 the highest separability occurred between black pine and masson pine and between black pine and slash pine with JM values of 2. The lowest separability occurred between slash pine and cedar (JM value of 1.0664). Among the ten pairs, JM values of six of them reached over 1.9 with a relatively high separability, as a whole.

Table 1: Population size of each species

Samples	Black pine	Masson pine	Slash pine	Cedar	*Pseudolarix*
Training samples	24	25	23	25	22
Verification samples	24	24	24	24	22
Total	48	49	47	49	44

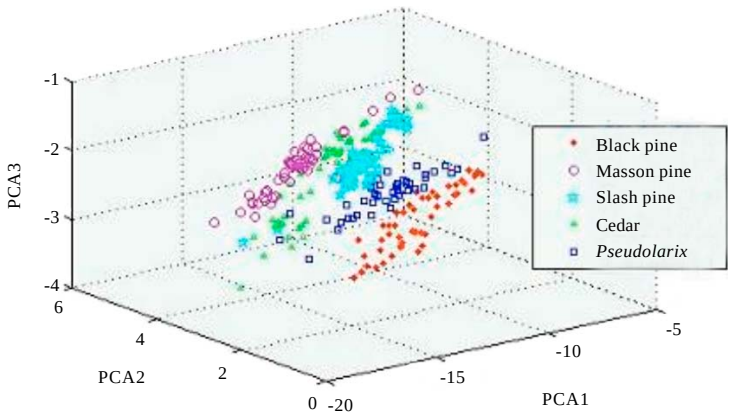

Fig. 4: Three-dimensional space diagram of 3 principal components of five coniferous tree species

Table 2: Jeffries-Matusita distance between any two of five coniferous tree species

Species pair	Jeffries-Matusita	Species pair	Jeffries-Matusita
Black pine/masson pine	2	Masson pine/cedar	1.2926
Black pine/slash pine	2	Masson pine/*Pseudolarix*	1.9998
Black pine/cedar	1.9999	Slash pine/cedar	1.0664
Black pine/*Pseudolarix*	1.6447	Slash pine *Pseudolarix*	1.9979
Masson pine/slash pine	1.8599	Cedar/*Pseudolarix*	1.9665

LAP-BP model: A three-layer structure was adopted for the neural network analysis: Input layer, hidden layer and output layer. The input layer had 3 neurons and the number of neurons of the output layer was the same as the number of classifications at 8 pieces. The principle for determining the output layer was as follows: (1) If the classification was in a corresponding position then the output value was 1, if it was in another position then it was set to 0. For example, the output values corresponding to black pine were [1, 0, 0, 0, 0, 0], (2) Furthermore, the output result was processed by utilizing a competition function in order to make the maximum output value of each pixel equal to 1, while the values for the others were set to 0. This allows us to avoid any impurities in our output results and also satisfies the hard classification of remote-sensing imaging. The activation function for determining both the hidden layer and the output layer was Laplace. SSE (error sum of squares) was adopted for error function. The learning rate (lr) was 0.5, the factor of momentum (mc) was 0.9 and the gradient factor was $\lambda = 0.5$, $u = 0$. Normalization processing was conducted for input data and the value range was [0, 1].

The number of neurons in the hidden layer, as well as the training objective, plays an important part in the predictive effect of neural networks. To date, there have been no methods found that can scientifically determine the number of hidden layers within an artificial neural network; most are done by trial and error. Meanwhile, the size of the network training objective (error) also greatly effects the predictive capability of the network. If the error it too big the predictive capability is poorer. Alternatively, if the error is too small (regardless of its strong predictive capability) overfitting may appear and generalization capability becomes very poor. Hence, selection of proper training objective is necessary. In this study, we set the range for both the hidden layer and the training objective in order to do a one-by-one search. Optimal combination of the hidden layer and the training objective was chosen based on the principle that the sum of

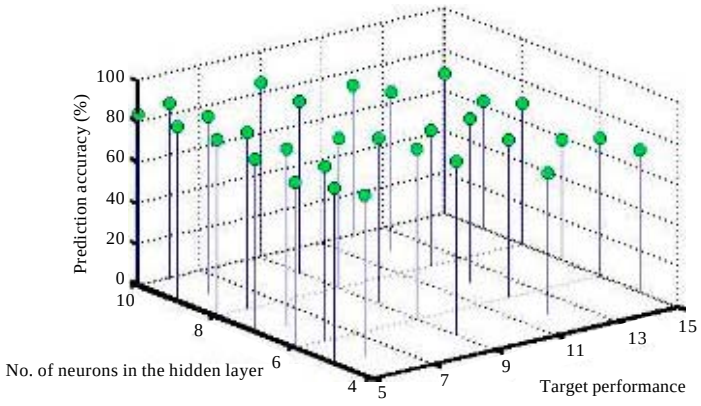

Fig. 5: Identification precision for five species of coniferous tree with different combinations of the hidden layer and the training objective

mean relative errors of both the prediction and the fitting were minimal. Furthermore, according to the total number of the training samples and the dimensions of the input and output layers, we: (1) Set the neuron range of the hidden layer as [5, 10] and increased it progressively by a step-length of 1 and (2) Set the range of the network training objective (i.e., the error sum of squares) to [15, 5] and increased it progressively by a step-length 2. Experimental results show that when the combination of the hidden layer and the training objective was (6, 9) the LAP-BP network had achieved the highest precision for coniferous tree species with a predictive precision of 86.78% (Fig. 5).

RESULTS AND DISCUSSION

According to Table 3, the identification rates for black pine, masson pine, slash pine, cedar and *Pseudolarix* were 87.5, 83.3, 79.2, 83.3 and 100%, respectively. The average JM distance between *Pseudolarix* and the other four tree species was 1.97 and the average JM distance between black pine and other four tree species was 1.91 which are the highest of all average the JM distances observed. Moreover, the experiment also showed that the identification rate for these two tree species was the highest. The average JM distance between slash pine and other four tree species was 1.73 which was the lowest of all of all of the JM distances. These results indicate that the identification rate for slash pine was the highest. Finally, the overall classification accuracy of all five coniferous species was 86.78%. The overall classification in this study is comparable to other findings. For example, the overall accuracy was near 90% for differentiating five conifers using spectral derivative technique and an artificial neural network (Gong *et al*., 1997). The back propagation neural-network classifier provided the best classification performance and was capable of classification accuracies of 97% (Burks *et al*., 2005). Those results implied that the back propagation neural-network classifier was good at species classification and achieved higher classification accuracy. In another hand, Support Vector Machine (SVM) algorithm produced overall accuracy 82.27% for six gregarious tree species (white oak, brown oak, chir pine, blue pine, cedar and fir in western Himalaya) classification (George *et al*., 2014). An overall correct classification rate of 0.72 was produced using different modeling techniques for mapping six major tree species (3 broadleaf and 3 conifers) in a study area of North-Eastern Switzerland (Engler *et al*., 2013). Compared the predictive power of the different classification techniques,

Table 3: Identification precision for five coniferous tree species

Species	Black pine	Masson pine	Slash pine	Cedar	*Pseudolarix*	User precision (%)
Black pine	21					100.0
Masson pine		20	1	3		83.3
Sash pine		2	19	1		86.4
Cedar		2	4	20		76.9
Pseudolarix	3				22	88.0
Producers accuracy (%)	87.5	83.3	79.2	83.3	100	

back propagation neural-network classifier generally performs better than other classification techniques, such as SVM.

The leaves of the five species of coniferous trees were also collected for comparative analysis using hyperspectral remote sensing. The leaf of the *Pseudolarix* had the highest identification rate and presented as linear, soft and flat; it was significantly different from the other four pine trees. The leaf of black pine was staunch and thick, as compared to the relatively slender needles of the other pines; the identification rate for black pine was also relatively high. From this data it can be concluded that the thickness and shape of the leaf is crucial for the identification of coniferous tree species based on hyperspectral data. The difference of leaf thickness and shape results in differences of reflectivity and transmittance by the sun, resulting in the observed spectral differences between the different coniferous tree species. Above conclusion also supported the result that the spectral properties are decided by the characteristics of forest species.

CONCLUSION

In this study, we discussed the identification of tree species based on hyperspectral analysis of their leaves. To achieve this goal we utilized a method that adapted the Laplace function as the activation function in order to improve the BP algorithm and then further integrated an improved neural network method that allowed us to discern between the five tree species studied. Results show that improving the activation function can raise the convergence rate of the neural network and moreover, that a very high precision can be achieved for differentiating tree species within a population via this method. Relative to published multi-spectral data, hyperspectral data presents with multiple, continuous bands and can provide much more information about the spectrum reflectivity for different tree species. These research results supply a strong reference for the theoretical support of hyperspectral remote-sensing and monitoring of a large area of forest in order to differentiate tree species via image data.

ACKNOWLEDGMENTS

This study was supported by the Forestry Commonweal Programs (No. 200904003) from State Forestry Administration, P.R. China.

REFERENCES

Burks, T.F., S.A. Shearer, J.R. Heath and K.D. Donohue, 2005. Evaluation of neural-network classifiers for weed species discrimination. Biosyst. Eng., 91: 293-304.

Dang, J., 2000. Neural Network Technology and Application. China Railway Publishing House, Beijing.

Engler, R., L.T. Waser, N.E. Zimmermann, M. Schaub, S. Berdos, C. Ginzler and A. Psomas, 2013. Combining ensemble modeling and remote sensing for mapping individual tree species at high spatial resolution. For. Ecol. Manage., 310: 64-73.

George, R., H. Padalia and S.P.S. Kushwaha, 2014. Forest tree species discrimination in western Himalaya using EO-1 Hyperion. Int. J. Applied Earth Observation Geoinformation, 28: 140-149.

Gong, P., R. Pu and B. Yu, 1997. Conifer species recognition: An exploratory analysis of *in situ* Hyperspectral data. Remote Sens. Environ., 62: 189-200.

Liu, X. and X. Zhang, 2004. Research development and strategy for remote-sensing classification of forest vegetation. For. Resour. Mange., 1: 61-64.

Martin, M.E., S.D. Newman, J.D. Aber and R.G. Congalton, 1998. Determining forest species composition using high spectral resolution remote sensing data. Remote Sens. Environ., 65: 249-254.

Pu, R. and P. Gong, 2000. Hyperspectral Remote Sensing and its Applications. Higher Education Press, Beijing.

Pu, R., G. Gong, R. Michishita and T. Sasagawa, 2008. Spectral mixture analysis for mapping abundance of urban surface components from the Terra/ASTER data. Remote Sens. Environ., 112: 939-954.

Qi, Y. and J. Zhang, 2007. Research on mixed pixel decomposition based on AGNNA. Anhui Agric. Sci. Bull., 13: 43-45.

Shen, Y. and B. Wang, 2003. A fast algorithm of neuron network with tunable activation function. Sci. China Series E: Technol. Sci., 33: 733-740.

Tan, B., 2003. Research discussion on application of hyperspectral remote-sensing to forestry. World For. Res., 16: 33-37.

Tan, B., Z. Li and E. Chen, 2005. Forest type identification of hyperspectral and multi-spectral remote-sensing data. J. Northeast For. Univ., 33: 61-64.

Tan, B., 2008. Research development of forest information extraction by hyperspectral remote-sensing. For. Res., 21: 105-111.

Wang, X. and Y. Zhang, 1998. AVHRR mixed pixel decomposition by neural network model. J. Remote Sens., 2: 51-56.

Wu, Y. and M. Zhao, 2001. TAF model and supervised learning and application. Sci. China Ser. E: Technol. Sci., 31: 263-272.

Wu, K., L. Zhang and P. Li, 2007. A mixed pixel decomposition method for network with varying end member. J. Remote Sens., 11: 20-26.

Yuan, Z., 1999. Artificial Neural Network and its Application. Tsinghua University Press, Beijing.

Zhang, L., L. Zheng and Q. Tong, 1997. The estimation of vegetation variables based on high resolution spectra. J. Remote Sens., 1: 111-114.

Zhang, Y. and M. Shao, 2002. Mixed pixel decomposition based on RBF neural network. J. Remote Sens., 6: 285-288.

Zhang, L. and L. Zhang, 2005. Hyperspectral Remote-Sensing. Wuhan University Press, Wuhan.

Zhang, G., 2007. Application and development of hyperspectral remote-sensing technology in modern agriculture. Sichuan For. Expl. Design, 4: 66-69.

Zhang, Y., Z. Wang and H. Wu, 2007. The Research of Application of Remote-Sensing Technology to Forest Resources Check. China Forestry Press, Beijing.

Zhang, L., K. Wu, Y. Zhong and P. Li, 2008. A new sub-pixel mapping algorithm based on a BP neural network with an observation model. Neurocomputing, 71: 2046-2054.

Zhao, S., 2003. Principle and Method of Remote-Sensing Application Analysis. Science Press, Beijing.